Research Square

Preprints are preliminary reports that have not undergone peer review.
They should not be considered conclusive, used to inform clinical practice,
or referenced by the media as validated information.

Regime Switching or Overdispersion: A Comparison of Poisson Hidden Markov and Negative Binomial Models for Annual Seismicity in Türkiye

Hakan Karaca

karaca26@hotmail.com

Niğde Ömer Halisdemir University

Research Article

Keywords: Hidden Markov model, Negative Binomial distribution, Poisson distribution, overdispersion, earthquake counts, Türkiye

Posted Date: November 18th, 2026

DOI: https://doi.org/10.21203/rs.3.rs-11119485/v1

License: This work is licensed under a Creative Commons Attribution 4.0 International License.
Read Full License

Additional Declarations: No competing interests reported.

Regime Switching or Overdispersion: A Comparison of Poisson Hidden Markov and Negative Binomial Models for Annual Seismicity in Türkiye

Hakan Karaca

Department of Architecture, Faculty of Architecture, Niğde Ömer Halisdemir University, Niğde, Türkiye

ORCID: https://orcid.org/0000-0003-3291-5822

Corresponding author: karaca26@hotmail.com

Abstract

Earthquake occurrence is a complex stochastic process characterized by temporal clustering, where periods of heightened seismic activity are frequently followed by aftershock sequences, leading to significant overdispersion in count data. This overdispersion — where the variance of earthquake counts substantially exceeds the mean — poses a challenge for standard Poisson-based modeling approaches, which assume equidispersion. Within this context, this study investigates the performance of Poisson Hidden Markov Models (PHMM) and Negative Binomial Hidden Markov Models (NBHMM) in capturing the latent regime-switching dynamics of earthquake frequency data in Türkiye, a region of high seismic activity situated at the intersection of major tectonic plates.

The results show that the two-state PHMM provides the best overall representation of the annual earthquake counts. Both AIC and BIC select this model; AIC provides stronger support, whereas BIC indicates that the one-state Negative Binomial model remains a competitive alternative. The stronger overall performance of the PHMM supports persistent changes between two statistical activity levels. Nevertheless, the competitive Negative Binomial fit indicates that within-state overdispersion also explains part of the observed variability. Thus, the Negative Binomial model provides a useful alternative interpretation, but it does not outperform the selected two-state PHMM.

Keywords: Hidden Markov model; Negative Binomial distribution; Poisson distribution; overdispersion; earthquake counts; Türkiye

Article Highlights

- Türkiye's annual earthquake counts alternate between two persistent statistical levels.
- A single overdispersed model remains a credible simpler explanation.
- Forecast tests show that both model families predict annual counts similarly.

1 Introduction

Earthquake occurrence is a complex stochastic process in which clustering and rate changes can influence the observed number of events (Gardner and Knopoff 1974; Ogata 1988). Consequently, annual earthquake counts may not be adequately represented by a single constant-rate model. One possible explanation is regime switching between statistical activity levels represented through Hidden Markov Models (HMMs). Distinguishing the governing patterns is important for selecting a defensible count model, although annual country-scale counts alone cannot establish distinct physical tectonic regimes.

HMMs offer a natural framework for exactly this kind of regime-dependent structure: they have emerged as a powerful tool for time series data that exhibit regime-switching behavior, where the underlying data-generating process alternates between a finite number of latent states (Rabiner 1989; Zucchini et al. 2016). In the context of seismology, HMMs are particularly well-suited to capturing the alternation between periods of varying seismic activity, as the latent states can naturally represent distinct seismic regimes. Earthquake counts within each regime are then modeled via an appropriate emission distribution, conditional on the underlying hidden state.

Hidden Markov models have been applied to seismicity in several settings (Chambers et al. 2012; Ebel et al. 2007; Orfanogiannaki et al. 2010). These studies do not all use the same observation model. Ebel et al. (2007) and Chambers et al. (2012), for example, modeled interevent-time and spatial information for mainshock forecasting, whereas Orfanogiannaki et al. (2010) used Poisson count emissions to identify discrete seismicity levels. Within Türkiye, Can et al. (2014) applied an HMM to earthquake occurrence in northwestern Türkiye. Count-emission models and models based on interevent times or spatial categories are therefore distinguished in the present review.

Among studies that model earthquake counts directly, PHMMs have been used to represent changes in the conditional event rate. Orfanogiannaki et al. (2010) showed how state-dependent Poisson emissions can partition a seismic record into statistically distinguishable states. More recently, PHMM's have been applied directly to regional earthquake time series in several settings. Orfanogiannaki et al. (2014) used a PHMM to analyze seismicity in Sumatra following the 2004 and 2005 earthquakes, finding that the two affected regions exhibited markedly different latent activity levels, consistent with stress transfer between them. Felix et al. (2022) applied a PHMM to nearly six decades of earthquake occurrences in Metro Manila, Philippines, identifying a five-state latent structure that outperformed ARIMA-based forecasts. Most recently, Georgakopoulou et al. (2024) employed PHMM across ten seismic zones in Central and South America, demonstrating improved probabilistic forecasting performance relative to classical Poisson models.

This literature motivates the PHMM as a model for persistent statistical regime patterns, but it does not imply that every HMM application to seismicity uses Poisson emissions. The Poisson distribution is a standard model for the number of events in a fixed interval when events occur independently at a constant rate; the associated exponential waiting-time model has the memoryless property (Cornell 1968; Gardner and Knopoff 1974; Kagan 2010; Luen and Stark 2012; Michael 2011; Shearer and Stark 2012). For a Poisson count, the conditional variance equals the conditional mean. Earthquake catalogues may depart from these assumptions because of clustering, rate heterogeneity or catalogue changes. Such departures can produce overdispersion, for which the variance exceeds the mean (Kagan 2010).

To address this limitation, the Negative Binomial (NB) distribution offers a natural generalization of the Poisson framework by introducing an additional dispersion parameter, allowing the variance to exceed the mean (Iturrieta et al. 2024; Kagan 2010; Taroni et al. 2023). This added flexibility makes the NBHMM a theoretically more appropriate candidate for modeling overdispersed count data such as earthquake frequencies (Iturrieta et al. 2024; Kagan 2010; Taroni et al. 2023). Despite this theoretical

advantage, the relative empirical performance of PHMM and NBHMM in the specific context of seismic activity in Türkiye has not been systematically investigated.

The present study applies the same HMM modelling, parameter-estimation, state-selection, and validation procedures to both Poisson HMM (PHMM) and Negative Binomial HMM (NBHMM) specifications to represent variations in annual earthquake counts across Türkiye. The analysis investigates whether the observed variability is better explained by persistent changes in latent mean-rate regimes, by within-state overdispersion, or by a combination of these mechanisms. Although multiple state configurations were evaluated for both model families, the model-selection criteria favoured a one-state Negative Binomial specification for the NBHMM family. Consequently, the final comparison is not simply between two alternative HMM emission distributions: it primarily contrasts the regime-switching structure identified by the PHMM with the overdispersion captured by the single-state Negative Binomial model. Their relative performance is further assessed through out-of-sample validation. The analysis is descriptive and probabilistic and is not intended as an operational earthquake forecasting or early-warning model.

2 Study area and data

Türkiye lies near the convergence of the Eurasian, Anatolian, Arabian, and African plates and contains several major active fault systems. Figure 1 presents earthquake epicenters with moment magnitude Mw ≥ 3.9 recorded between 1976 and 2025, together with mapped active fault traces. Seismicity is spatially heterogeneous, with concentrations in western Anatolia, along the North Anatolian Fault corridor, and in eastern and southeastern Türkiye (Barka 1996; Stein et al. 1997). Because the analysis aggregates these tectonically distinct regions into annual national counts, the inferred hidden states are interpreted as statistical count regimes rather than direct physical tectonic states.

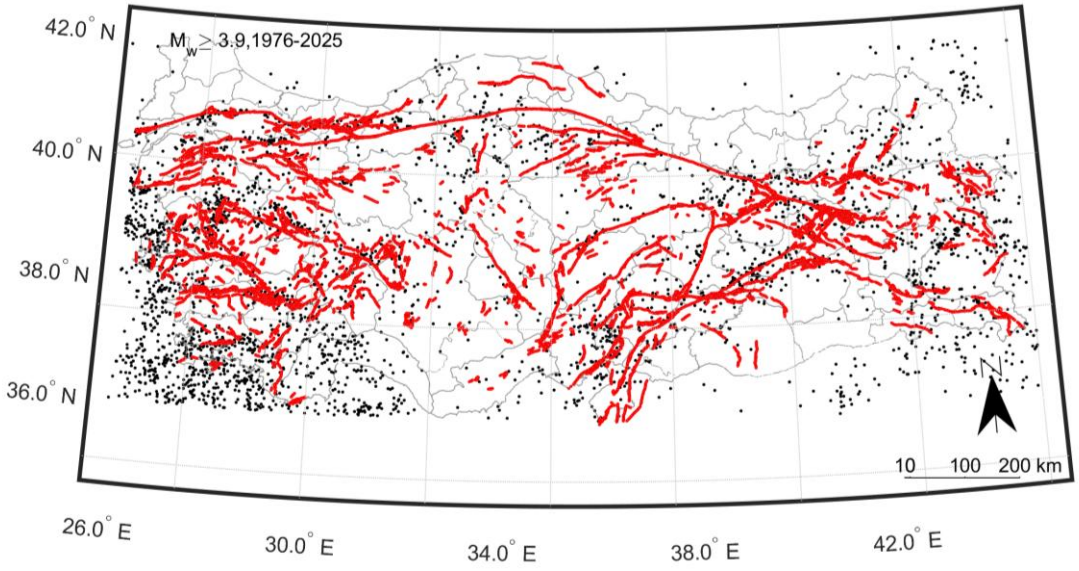


Fig. 1 Spatial distribution of earthquake epicenters (Mw ≥ 3.9, 1976–2025) and major active fault traces across Türkiye. Black dots represent earthquake epicenters; red lines indicate mapped active fault segments. The study area spans 26°E–45°E and 36°N–42°N

The earthquake catalogue was obtained from the Kandilli Observatory and Earthquake Research Institute (KOERI). Before analysis, reported magnitudes were converted to moment magnitude (Mw) using empirical relationships developed for Turkish seismic data (Akkar and Çağnan 2010; Ulusay et al. 2004). The homogenized catalogue was declustered using the conventional space–time window method

of Gardner and Knopoff (1974) to reduce the influence of foreshock and aftershock sequences. Catalogue completeness was assessed using a magnitude–time (Mc–t) plot (Figure 2). The analysis indicates that Mc stabilizes at approximately Mw 3.9 from 1976 onward, after greater fluctuation during 1971–1975 associated with more limited early network coverage. The study period was therefore defined as 1976–2025, and events satisfying Mw ≥ 3.9 were retained. The time-dependent completeness curve is used here as a screening diagnostic and does not imply perfect catalogue homogeneity.

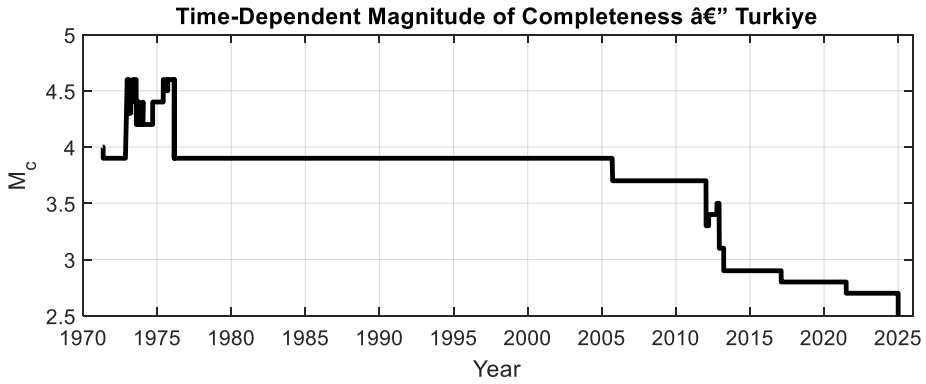


Fig. 2 Time-dependent magnitude of completeness (Mc) for the Türkiye earthquake catalogue (1971–2025), estimated using the Cao and Gao (2002) procedure

Figure 3 displays the annual number of retained earthquakes for 1976–2025. The series shows substantial year-to-year variation and multi-year intervals of comparatively lower and higher counts. The observed temporal pattern motivates comparing persistent changes in the conditional mean with a single-regime model that accommodates overdispersion.

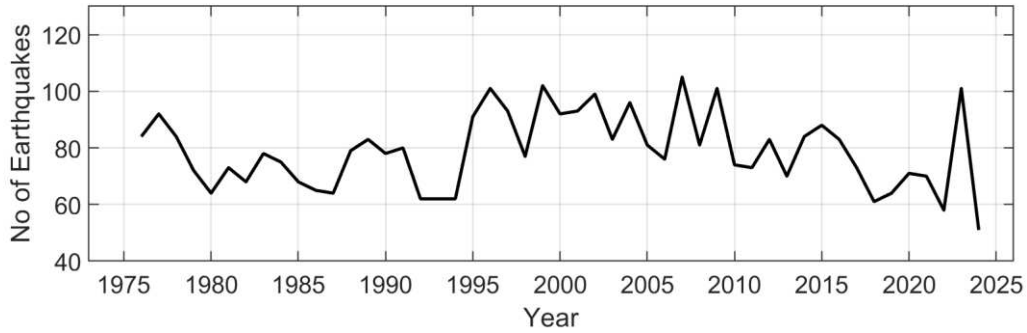


Fig. 3 Annual number of earthquakes (Mw ≥ 3.9) in Türkiye, 1976–2025, derived from the declustered KOERI earthquake catalogue

As a preliminary trend diagnostic, Table 1 reports the Mann–Kendall test and Sen's slope for the 50 annual counts. No statistically significant monotonic trend is detected (p = .688), and the estimated slope is −0.04 events/year with a 95% confidence interval that includes zero. This result indicates a lack of evidence for a monotonic trend; it does not establish stationarity or exclude structural changes, nonlinear trends, or changes in variance.

Table 1 Mann-Kendall trend test and Sen's slope estimator for the annual earthquake count series (1976–2025, T = 50)

Mann-Kendall					Sen's Slope	
S	**Var(S)**	**Z**	**p**	**Kendall's τ**	**Sen's slope**	**Sen's slope 95% CI**
-49	14,253.67	−0.40	0.688	−0.04	−0.04 events/year	[−0.33, 0.25]

To assess the adequacy of the Poisson equidispersion assumption prior to model fitting, the dispersion index (sample variance/mean) of the annual earthquake count series was computed as 2.19, indicating that the variance exceeds the mean by more than a factor of two. A preliminary method-of-moments calculation gives r ≈ 66.3. This value is a descriptive estimate based directly on the sample moments and is distinguished from the maximum-likelihood dispersion estimate of the fitted one-state Negative Binomial model reported in the Results section.

3 Methodology

Count-based time series, such as earthquake occurrence data, are commonly modeled using the Poisson distribution due to its simplicity and well-established theoretical properties. However, the Poisson model imposes the restrictive assumption of equidispersion (i.e., mean equal to variance), which is frequently violated in seismic catalogs due to spatial and temporal clustering of events. To account for this overdispersion, the NB distribution is adopted as a more flexible alternative, as it explicitly allows the variance to exceed the mean. The primary distinction lies in the treatment of variance. While the Poisson model assumes a fixed rate parameter λ, the Negative Binomial model can be interpreted as a Poisson–Gamma mixture, in which λ itself is treated as a random variable following a Gamma distribution (Table 2).

Table 2 Probability mass functions and principal properties of the count distributions

Distribution	**Probability Mass Function**	**Mean**	**Standard Deviation**
Poisson	$f(x) = \frac{\lambda^x e^{-\lambda}}{x!}$	λ	$\sqrt{\lambda}$
Negative Binomial	$f(x) = \frac{\Gamma(x+r)}{\Gamma(r)x!} \cdot \left(\frac{r}{r+\mu}\right)^r \cdot \left(\frac{\mu}{r+\mu}\right)^x$	μ	$\sqrt{\mu + \frac{\mu^2}{r}}$

This formulation accommodates unobserved heterogeneity in the event rate. In the present national-scale series, such heterogeneity may reflect temporal rate variation, aggregation across tectonic regions, monitoring changes, declustering choices, or other unmodeled factors. The Negative Binomial model therefore provides a flexible statistical description of overdispersed counts; it should not be interpreted as identifying a unique physical source of that overdispersion.

$\{S_t\}_{t=1}^{T}\{1, 2, \ldots, K\}K$Both distributions are considered within a hidden-state modeling framework, but the interpretation depends on the selected number of states. An HMM consists of an unobserved state sequence and observations whose conditional distribution depends on the current state (Rabiner, 1989; Zucchini et al., 2016). Let the latent process be a discrete-time, first-order Markov chain with K states, and let the annual count be conditionally distributed according to a state-specific Poisson or Negative Binomial probability mass function. When K = 1, the model contains no hidden-state transitions and reduces to an ordinary single-regime count model.

$$\pi = (\pi_1, \ldots, \pi_K) \tag{1}$$

where $\pi_i = P(S_1 = i)$ and A transition probability matrix

$$\boldsymbol{A} = \{a_{ij}\}, a_{ij} = P(S_t = j \mid S_{t-1} = i) \tag{2}$$

$Y_t tt = 1, \ldots, TT = 50 S_t = kY_t f(y_t; \mid S_t = k\theta_k) S_t \Lambda = (\boldsymbol{\pi}, \boldsymbol{A}, \boldsymbol{\theta})$The transition probabilities satisfy the usual row-sum constraint. Let the observed sequence contain T = 50 annual counts for 1976–2025. Conditional on the hidden state, each annual count follows its state-specific emission distribution. The likelihood sums over all possible hidden-state sequences and is evaluated using the forward algorithm.

$$P(Y_1, \ldots, Y_T \mid \Lambda) = \sum_{s_1, \ldots, s_T} \pi_{s_1} f(y_1 \mid \theta_{s_1}) \prod_{t=2}^{T} a_{s_{t-1} s_t} f(y_t \mid \theta_{s_t}) \tag{3}$$

$K^T f(y_t \mid \theta_k)$Two emission specifications are examined: Poisson and Negative Binomial. The principal empirical comparison is between the selected two-state PHMM and the selected one-state Negative Binomial model. The latter is referred to as a Negative Binomial model rather than an NBHMM when discussing the final K = 1 specification, because it contains no regime-switching mechanism.

$\Lambda = (\pi, A, \theta) K$Model parameters were estimated by maximum likelihood using the Baum–Welch expectation–maximization algorithm (Baum et al., 1970; Rabiner, 1989). Candidate models with K = 1–4 states were fitted. Because the annual series contains only 50 observations and parameter counts increase rapidly with K, models with more than four states were not considered, and results for K = 3–4 are interpreted cautiously. State labels were ordered by increasing fitted mean to reduce label ambiguity, and the converged solution with the largest maximized log-likelihood was retained for each candidate specification. All computational settings used for estimation are preserved in the accompanying MATLAB analysis files.

The relative performance of PHMM and NBHMM is assessed using complementary information criteria. The Akaike Information Criterion (AIC; Akaike 1974) is defined as:

$$\text{AIC} = -2\,\ell(\widehat{\Lambda}) + 2p \tag{4}$$

The Bayesian Information Criterion (BIC; Schwarz 1978) is defined as:

$$\text{BIC} = -2\,\ell(\widehat{\Lambda}) + p\ln(T) \tag{5}$$

where $\ell(\widehat{\Lambda})$ is the maximized log-likelihood and p is the number of free parameters in the model. Because the NBHMM includes K additional dispersion parameters relative to the PHMM, both criteria penalize the added complexity of the NBHMM, ensuring that any improvement in fit is not merely a product of increased model flexibility. Lower AIC/BIC values indicate a preferred model.

$\hat{s}_1, \ldots, \hat{s}_T P(S_{1:T}, = s_{1:T} \mid Y_{1:T} \mid \widehat{\Lambda})$After estimation, the Viterbi algorithm was used to obtain the single most likely state sequence. The decoded sequence is a convenient summary but does not express classification uncertainty; smoothed state probabilities should therefore accompany the Viterbi path in an expanded diagnostic analysis. All analyses were implemented in MATLAB 2018.

4 Results and discussion

This section presents the results obtained from fitting the Poisson and Negative Binomial count specifications within the common HMM framework. Candidate models containing one to four states are first compared using maximized log-likelihood, AIC, and BIC to examine the balance between goodness of fit and model complexity. The emission parameters and, where applicable, transition probabilities of the principal models are then evaluated to characterize how each specification represents the observed variability in annual earthquake counts. Parameter uncertainty is subsequently examined through bootstrap analysis, while rolling-origin and block-holdout procedures are used to assess out-of-sample predictive performance. Finally, the results are considered collectively to determine the relative roles of latent state changes and within-state overdispersion in representing annual seismicity.

Figure 4 summarizes the trade-off between fitting performance and complexity. Log-likelihood increases as the number of states grows, but AIC and BIC penalize the additional parameters and both select the two-state PHMM. The one-state Negative Binomial model begins with a substantially better fit than the one-state Poisson model because its dispersion parameter accommodates excess variance without state switching. The crossing pattern therefore illustrates the central comparison: persistent changes in the conditional mean versus within-state overdispersion. Given number of considered years is 50, the higher-state models should be viewed cautiously because their parameter estimates are more vulnerable to weak identification and local optima.

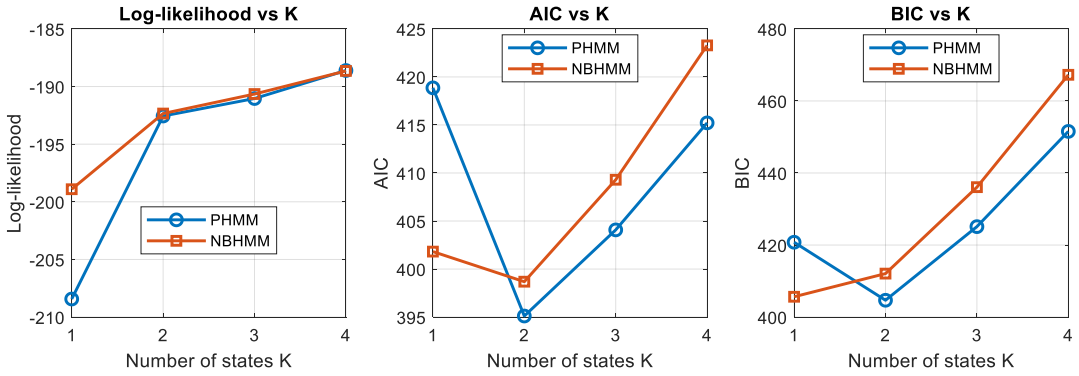


Fig. 4 Log-likelihood, AIC, and BIC as a function of the number of hidden states (K), for the Poisson-HMM (PHMM) and Negative Binomial-HMM (NBHMM)

Table 3 summarizes model selection for K = 1–4 states. The two-state PHMM has the lowest AIC and BIC, relative to the one-state Negative Binomial model, the AIC difference is 6.71, providing clearer support for the PHMM under AIC, whereas the BIC difference is only 0.97 and therefore does not provide decisive evidence between the two explanations (see Table 3). Models with $K \geq 3$ receive no support from either criterion. The two-state PHMM and one-state Negative Binomial model are consequently carried forward as the principal alternatives, with the two-state NBHMM retained as a secondary reference in out-of-sample comparisons reported in Table 6.

Table 3 Model selection criteria (log-likelihood, number of parameters, AIC, BIC) for PHMM and NBHMM as a function of the number of hidden states, K

	PHMM				NBHMM			
State	**n**	**LL**	**AIC**	**BIC**	**n**	**LL**	**AIC**	**BIC**
1	1	-208.43	418.86	420.78	2	-198.91	401.82	405.64

2	5	-192.56	395.11	404.67	7	-192.49	398.99	412.37
3	11	-191.04	404.08	425.11	14	-191.84	411.67	438.44
4	19	-188.61	415.22	451.55	23	-189.4	424.81	468.78

Figure 5 contrasts the temporal representations produced by the two principal models. The PHMM assigns years to lower- and higher-count statistical states with fitted means of approximately 70.44 and 89.66 events/year. The one-state Negative Binomial model has no hidden-state decomposition and represents the observed variation through a single mean and an additional dispersion parameter. The BIC values differ by only 0.97, whereas AIC more clearly favors the PHMM. Accordingly, the models are not described as statistically equivalent: the evidence is criterion-dependent, with the PHMM preferred overall, while the simpler overdispersion-based explanation remains competitive under BIC. The decoded PHMM states represent statistical classifications and should not be interpreted as direct tectonic regimes.

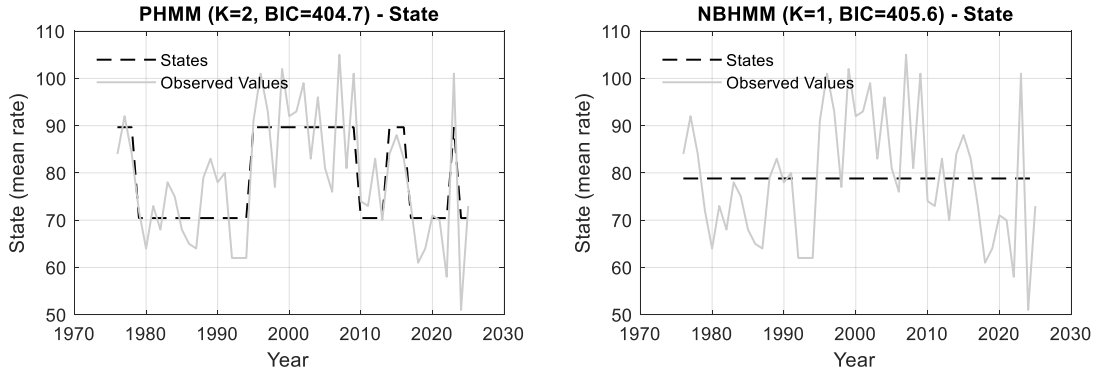


Fig. 5 Decoded hidden-state sequence (dashed line) against the observed annual earthquake counts (solid grey), for the PHMM (K = 2, BIC = 404.7) and the one-state Negative Binomial model (BIC = 405.6)

Table 4 characterizes the fitted count distributions. The PHMM decoding assigns 28 of 50 years to a lower-count state (mean = 70.44 events/year) and 22 years to a higher-count state (mean = 89.66 events/year). Under the Poisson specification, the conditional variance equals the conditional mean. The one-state Negative Binomial model instead estimates a mean of 78.82 and variance of 169.13. Thus, the alternatives (PHMM and NBHMM) represent aggregate overdispersion through different statistical mechanisms: between-state variation in the PHMM and within-state variation in the NB model.

Table 4 PHMM and Negative Binomial emission parameters

	PHMM			**Negative Binomial**		
Hidden State	**Duration**	**Mean, m (eq/year)**	**Variance**	**Duration**	**Mean, m (eq/year)**	**Variance**
1	28	70.44	70.44	50	78.82	169.13
2	22	89.66	89.66			

Table 5 reports the fitted transition matrix for the two-state PHMM. The diagonal probabilities (0.880 and 0.806) indicate persistence in the decoded statistical count states. The expected durations are approximately 8.3 and 5.2 years, respectively. These estimates describe persistence in the fitted model; though the estimated transition pattern does not represent the physical expansion or dissipation of tectonic activity. Figure 5 shows the associated switch probabilities between the in-state transition and state-to-state transition.

Table 5 Estimated transition probability matrix for the PHMM (K = 2)

	State 1 (low, μ=70.44)	**State 2 (high, μ=89.66)**
State 1 (low)	**0.880**	**0.120**
State 2 (high)	0.194	0.806

The identification of persistent low- and high-seismicity levels indicates the presence of statistically distinct activity states. The present analysis extends previous seismic HMM applications (see Sect. 1) by demonstrating that, for annual Türkiye-wide earthquake counts, a two-state Poisson representation should be evaluated alongside a competitive single-state model that accounts for overdispersion.

Figure 6 shows bootstrap distributions for the PHMM state means and transition probabilities. The intervals for the fitted state means do not overlap in the bootstrap sample, whereas the transition-probability intervals are wider, consistent with the small number of inferred switches in a 50-year series. This supports distinguishable statistical count levels within the fitted model, but it does not eliminate uncertainty about state classification or justify direct physical regime interpretation.

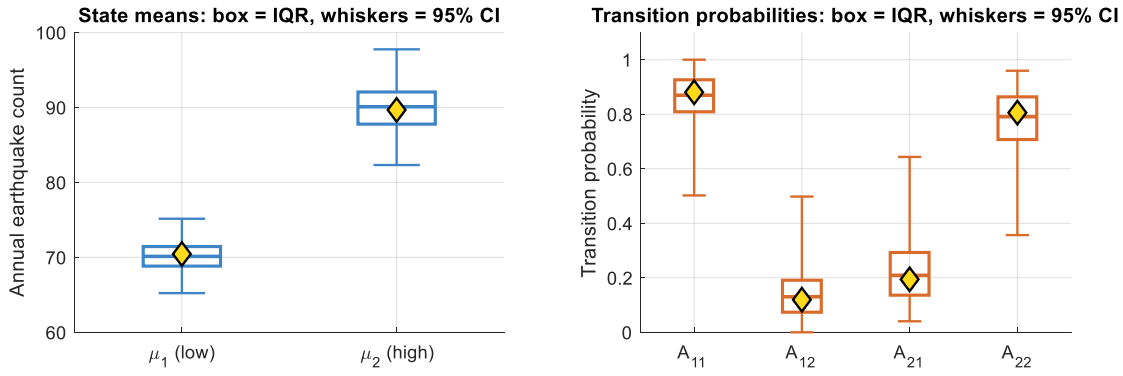


Fig. 6 Bootstrap distributions of the PHMM (K = 2) state means (left) and transition probabilities (right). The boxes indicate interquartile ranges, lines extending from the boxes represent 95% confidence intervals, and yellow diamonds indicate point estimates from the observed data

Table 6 reports out-of-sample predictive log-likelihoods for the three retained specifications. Under rolling-origin validation, total log scores differ by less than one unit across 25 held-out years; block-holdout ordering favors the one-state NB model. A paired t-test was used to compare the annual rolling-origin log scores of the two-state PHMM and the one-state NB model. The difference was not statistically significant (t=0.04, p=.97, n=25), indicating that neither model showed a systematic predictive advantage over the validation period. Because the annual score differences may be serially dependent, this result is interpreted descriptively rather than as evidence of predictive equivalence.

Table 6 Out-of-sample predictive log-likelihood under rolling-origin and block-holdout validation (1976–2025 series, T = 50)

Model	**Rolling Origin (2001 – 2025) (n=25)**	**Block-holdout (2010-2025) (n=16)**
PHMM (K=2)	-102.31	-67.55
Negative Binomial (K=1)	-102.45	-65.35
NBHMM (K=2)	-101.65	-66.71

Figure 7 displays one-step-ahead conditional predictive intervals for the 16 block-holdout years. Eleven of the 16 observations fall within the nominal 80% predictive intervals, corresponding to an empirical coverage rate of 68.75%. However, the exact 95% binomial confidence interval for the underlying coverage probability ranges from 41.3% to 89.0%. Because the interval includes 80%, there is no clear evidence that the model systematically underestimates uncertainty. The intervals condition on fitted parameters unless parameter uncertainty was incorporated in their construction. The 2023 and 2024 counts fall outside the displayed bounds, but the 2023 miss cannot be attributed specifically to retained aftershocks of Maras earthquakes without an event-level audit of the declustered catalogue.

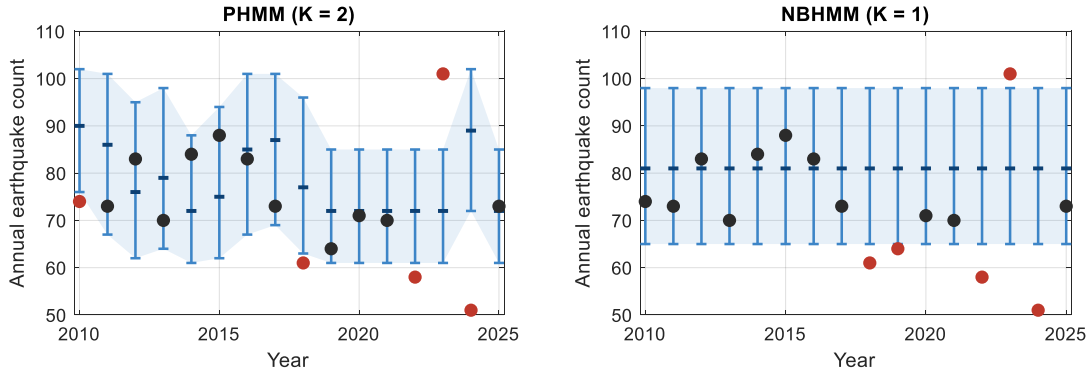


Fig. 7 One-step-ahead conditional 10th–50th–90th percentile predictive intervals for the block-holdout years (2010–2025), shown for the PHMM (K = 2, left) and one-state Negative Binomial model (right). Vertical bars show the [P10, P90] interval, median ticks show P50, black dots indicate observations within the interval, and red dots indicate observations outside it

Overall, both AIC and BIC select the two-state PHMM. The AIC difference of 6.71 provides clear support for the PHMM, whereas the BIC difference of 0.97 indicates that the one-state Negative Binomial model remains a competitive alternative. The Mann–Kendall test shows no significant monotonic trend in the annual earthquake counts. Bootstrap results support the separation of the two PHMM count levels and confirm the persistence of the identified statistical states. Out-of-sample validation also shows comparable predictive performance among the principal models. Taken together, these findings indicate that regime switching provides the strongest overall representation of annual seismicity, while within-state overdispersion offers a credible alternative explanation. The identified states should therefore be interpreted as persistent statistical count regimes that provide a useful probabilistic description of temporal variations in earthquake activity across Türkiye.

5 Conclusions

This study examined whether the variability in 50 annual earthquake counts from the declustered Türkiye catalogue (Mw ≥ 3.9, 1976–2025) is better represented by transitions between persistent count regimes. Applying the same estimation, state-selection, and validation procedures to Poisson and Negative Binomial specifications provided a direct comparison of these two statistical models. The results show that the two-state PHMM provides the strongest overall representation of the observed annual seismicity by balancing goodness of fit and model complexity.

Both AIC and BIC select the two-state PHMM. The ΔAIC value of 6.71 provides clear support for the PHMM over the one-state Negative Binomial model, while the smaller ΔBIC value of 0.97 indicates that overdispersion remains a credible alternative explanation. This difference between the criteria is

informative: the temporal variability in annual earthquake counts contains evidence of persistent changes in the conditional mean, although part of the same variability can also be represented through a single overdispersed count distribution.

The PHMM identifies two clearly separated statistical activity levels, with mean annual counts of approximately 70 and 90 earthquakes. The high diagonal transition probabilities and corresponding mean state durations of approximately 8.3 and 5.2 years indicate that these levels persist over multiple years rather than representing isolated annual fluctuations. Bootstrap results further support the separation of the state-dependent means. At the same time, the small out-of-sample log-score differences show that both regime switching and within-state overdispersion capture important features of the observed count variability.

The principal contribution of this study is therefore to demonstrate that annual seismicity across Türkiye cannot be fully characterized as random variation around a single constant Poisson rate. A regime-switching Poisson structure provides the best-supported statistical description, while the competitive Negative Binomial model confirms that excess variability is a fundamental feature of the series. The inferred states should be interpreted as persistent statistical count regimes rather than direct tectonic states; nevertheless, they provide a meaningful probabilistic framework for characterizing temporal changes in earthquake activity at the national scale.

Statements and Declarations

Funding
The author received no specific funding for this work.

Competing interests
The author declares no competing interests.

Author contributions
Hakan Karaca: Conceptualization, methodology, software, validation, formal analysis, investigation, data curation, visualization, writing—original draft, and writing—review and editing.

Ethics approval
Not applicable.

Acknowledgments
The author acknowledges the Kandilli Observatory and Earthquake Research Institute for providing the earthquake catalogue used in this study.

Data availability
The earthquake catalogue is publicly available from the Kandilli Observatory and Earthquake Research Institute (KOERI). The processed annual-count series supporting the findings of this study is available from the corresponding author upon reasonable request.

Code availability
The MATLAB code used for model fitting, validation, and figure generation is available from the corresponding author upon reasonable request.

References

Akaike H (1974) A new look at the statistical model identification. IEEE Trans Autom Control 19:716–723. https://doi.org/10.1109/TAC.1974.1100705

Akkar S, Çağnan Z (2010) A local ground-motion predictive model for Türkiye and its comparison with other regional and global ground-motion models. Bull Seismol Soc Am 100:2978–2995. https://doi.org/10.1785/0120090367

Barka AA (1996) Slip distribution along the North Anatolian fault associated with the large earthquakes of the period 1939 to 1967. Bull Seismol Soc Am 86:1238–1254

Baum LE, Petrie T, Soules G, Weiss N (1970) A maximization technique occurring in the statistical analysis of probabilistic functions of Markov chains. Ann Math Stat 41:164–171. https://doi.org/10.1214/aoms/1177697196

Can CE, Ergun G, Gokceoglu C (2014) Prediction of earthquake hazard by hidden Markov model (around Bilecik, NW Türkiye). Cent Eur J Geosci 6:403–414. https://doi.org/10.2478/s13533-012-0180-1

Cao A, Gao SS (2002) Temporal variation of seismic b-values beneath northeastern Japan island arc. Geophys Res Lett 29. https://doi.org/10.1029/2001GL013775

Chambers DW, Baglivo JA, Ebel JE, Kafka AL (2012) Earthquake forecasting using hidden Markov models. Pure Appl Geophys 169:625–639. https://doi.org/10.1007/s00024-011-0315-1

Cornell CA (1968) Engineering seismic risk analysis. Bull Seismol Soc Am 58:1583–1606. https://doi.org/10.1785/BSSA0580051583

Ebel JE, Chambers DW, Kafka AL, Baglivo JA (2007) Non-Poissonian earthquake clustering and the hidden Markov model as bases for earthquake forecasting in California. Seismol Res Lett 78:57–65. https://doi.org/10.1785/gssrl.78.1.57

Felix EFO, Buhat CAH, Mamplata JB (2022) Poisson hidden Markov model on earthquake occurrences in Metro Manila, Philippines. Earth Sci Inform 15:1635–1645. https://doi.org/10.1007/s12145-022-00810-x

Gardner JK, Knopoff L (1974) Is the sequence of earthquakes in Southern California, with aftershocks removed, Poissonian? Bull Seismol Soc Am 64:1363–1367

Georgakopoulou E, Tsapanos TM, Makrides A, Scordilis E, Karagrigoriou A, Papadopoulou A, Karastathis V (2024) Seismic evaluation based on Poisson hidden Markov models—the case of Central and South America. Stats 7:777–792. https://doi.org/10.3390/stats7030047

Iturrieta PC, Gerstenberger MC, Rollins C, Van Dissen R, Wang T, Schorlemmer D (2024) Implementing non-Poissonian forecasts of distributed seismicity into the 2022 Aotearoa New Zealand National Seismic Hazard Model. Bull Seismol Soc Am 114:244–257. https://doi.org/10.1785/0120230168

Kagan YY (2010) Statistical distributions of earthquake numbers: consequence of branching process. Geophys J Int 180:1313–1328. https://doi.org/10.1111/j.1365-246X.2009.04487.x

Kandilli Observatory and Earthquake Research Institute (KOERI) (2026) Earthquake database. http://www.koeri.boun.edu.tr/sismo/zeqdb/. Accessed September 2026

Luen B, Stark PB (2012) Poisson tests of declustered catalogues. Geophys J Int 189:691–700. https://doi.org/10.1111/j.1365-246X.2012.05400.x

Michael AJ (2011) Random variability explains apparent global clustering of large earthquakes. Geophys Res Lett 38:L21301. https://doi.org/10.1029/2011GL049443

Ogata Y (1988) Statistical models for earthquake occurrences and residual analysis for point processes. J Am Stat Assoc 83:9–27. https://doi.org/10.1080/01621459.1988.10478560

Orfanogiannaki K, Karlis D, Papadopoulos GA (2010) Identifying seismicity levels via Poisson hidden Markov models. Pure Appl Geophys 167:919–931. https://doi.org/10.1007/s00024-010-0088-y

Orfanogiannaki K, Karlis D, Papadopoulos GA (2014) Identification of temporal patterns in the seismicity of Sumatra using Poisson hidden Markov models. Res Geophys 4:4969. https://doi.org/10.4081/rg.2014.4969

Rabiner LR (1989) A tutorial on hidden Markov models and selected applications in speech recognition. Proc IEEE 77:257–286. https://doi.org/10.1109/5.18626

Schwarz G (1978) Estimating the dimension of a model. Ann Stat 6:461–464. https://doi.org/10.1214/aos/1176344136

Shearer PM, Stark PB (2012) Global risk of big earthquakes has not recently increased. Proc Natl Acad Sci USA 109:717–721. https://doi.org/10.1073/pnas.1118525109

Stein RS, Barka AA, Dieterich JH (1997) Progressive failure on the North Anatolian fault since 1939 by earthquake stress triggering. Geophys J Int 128:594–604. https://doi.org/10.1111/j.1365-246X.1997.tb05321.x

Taroni M, Spassiani I, Laskin N, Barani S (2023) How many strong earthquakes will there be tomorrow? Front Appl Math Stat 9:1152476. https://doi.org/10.3389/fams.2023.1152476

Ulusay R, Tuncay E, Sönmez H, Gökçeoğlu C (2004) An attenuation relationship based on Turkish strong motion data and iso-acceleration map of Türkiye. Eng Geol 74:265–291

Zucchini W, MacDonald IL, Langrock R (2016) Hidden Markov models for time series: an introduction using R, 2nd edn. Chapman and Hall/CRC, Boca Raton. https://doi.org/10.1201/b20790